European **Rev**iew for **Med**ical and **Pharmacol**ogical **Sci**ences 2019; 23: 8971-8983

LncRNA SNHG1 contributes to tumorigenesis and mechanism by targeting miR-338-3p to regulate PLK4 in human neuroblastoma

N. ZHANG, F.-L. LIU, T.-S. MA, Z.-D. ZENG. J.-J. ZHANG

Department of Neonatal Surgery, XuZhou Children's Hospital, Quan Shan District, Xuzhou, Jiangsu Province, China

Abstract. – OBJECTIVE: Neuroblastoma is a common malignancy in children. Despite the occurrence of diverse therapies in recent years, the survival rate of patients with high-risk NB is still unpredictable due to the high metastatic potential and poor prognosis. Therefore, it is urgent to study the molecular mechanism of NB metastasis. SNHG1 has been reported to be closely related to the development, metastasis, and prognosis of many cancers. The purpose of this study was to clarify the molecular mechanism of the role of SNHG1 in NB tumors.

PATIENTS AND METHODS: The expression levels of SNHG1, miR-338-3p, and PLK4 were detected by quantitative Real Time-Polymerase Chain Reaction (qRT-PCR) and Western blot, respectively. The functional targets between miR-338-3p and SNHG1 or PLK4 were predicted by online software Diana tools and observed by Luciferase reporter assay and RIP assay. Cell proliferation was measured by MTT assay. Cell migration and invasion were operated through flow cytometry. The expression of p-AKT was quantified by Western blot. Xenograft tumor model was established to confirm the biological role of SNHG1 in NB *in vivo*.

RESULTS: The expression levels of SNHG1 and PLK4 were increased in NB tissues and cells, and miR-338-3p expression was on the contrary. PLK4 was verified as a direct target of miR-338-3p and miR-338-3p could specially bind to SNHG1. The negative effect of SNHG1 down-regulation on cell proliferation, migration, and invasion could be rescued by miR-338-3p inhibition. The suppression of miR-338-3p mimics on cell proliferation, migration, and invasion could be reversed by PLK4 overexpression. In addition, SNHG1 knockdown weakened the volume and weight of tumor *in vivo*.

CONCLUSIONS: SNHG1 conduced to tumorigenesis and mechanism by upregulating PLK4 and by acting as miR-338-3p sponge in neuroblastoma.

Key Words:
Neuroblastoma, LncRNA SNHG1, MiR-338-3p, PLK4.

Abbreviations

NB, Neuroblastoma; lncRNAs, long non-coding RNAs; SNHG1, small nucleolar RNA host gene 1 (SNHG1); CRC, colorectal cancer; HCC, Hepatocellular carcinoma; NSCLC, non-small cell lung cancer; SMO, smoothened gene.

Introduction

Neuroblastoma (NB), the extremely heterogeneous disease both in biology and clinic, is the most common embryonal tumor of the autonomic nervous system in childhood[1,2]. NB tumors are controlled easily and can be cured with chemotherapeutic drugs and irradiation at early stage. However, NB tumors are mightily metastatic and often become resistant to chemotherapy and irradiation at advanced stage[2]. The investigation showed that more than 50% of all NB patients were diagnosed with metastatic diseases[3]. Metastatic disease remains an enormous challenge in the treatment of NB. Although the transplantation modalities on NB have evident improvement, the prognosis still is known as pessimistic for high-risk NB patients[4]. Therefore, research on the molecular mechanism of NB tumor metastasis remains an important issue.

Long non-coding RNAs (lncRNAs), greater than 200 nucleotides in length, are defined as transcribed RNA molecules[5]. LncRNAs widely contribute to the occurrence and development of numerous diseases and cancers as important functional roles[6]. Small nucleolar RNA host gene 1 (SNHG1), which is localized at 11q12.3 and has 11 exons[7], is identified as one kind of lncRNAs. It serves as a key role in the development and prognosis of numerous cancers. For example, the study showed that SNHG1 had a higher ex-

Corresponding Author: Fengli Liu, MD; e-mail: jindayongychmp@163.com

pression in colorectal cancer (CRC) and acted as an oncogene in CRC through Wnt/β-catenin pathway[8]. SNHG1 was highly expressed in hepatocellular carcinoma (HCC) and was contributed to cell proliferation by inhibiting the expression of p53 and p53-target genes BAX, FAS, and CDKN1A[7]. Cui et al[9] found that SNHG1 accelerated non-small cell lung cancer (NSCLC) tumorigenesis and growth through miR-101-3p/SOX9/Wnt/β-catenin axis and its overexpression was significantly associated with lower overall survival. However, the research on neuroblastoma of SNHG1 was limited.

MicroRNAs (miRs) are always the focus of researchers and have been confirmed as important contributors in complex gene regulation networks and various aspects of human disease[10]. MiR-338-3p was localized at 17q25.3 and has 22 nucleotides[11]. The research of miR-338-3p on various cancers has aroused much attention. Huang et al[12] found that miR-338-3p had negative effect on cell migration and invasion by targeting smoothened gene (SMO) in liver cancer. Chen et al[13] showed that miR-338-3p downregulation could enhance N-cadherin expression and SMO-mediated activation of the SHH/Snail1 pathway, then resulting in epithelial-mesenchymal transition (EMT). Huang et al[14] indicated that miR-338-3p suppressed the progression of EMT by regulating ZEB2 and MACC1/Met/Akt signaling in gastric cancer (GC) cells, which evidenced that miR-338-3p restrains cell migration and invasion in cancer. These results provide a valuable reference for our research in NB. Polo-like kinases (plks) are components of the complex cell development and impact multiple aspects in cell cycle progression[15]. PLK4 maps to a chromosome region, 4q28[16], and plays a unique role in centrosome duplication[17]. Several previous studies had been demonstrated to enhance cancer cell invasion. Lohse et al[18] suggested that CFI-400945 acted as PLK4 inhibition, and could significantly reduce tutor growth and increase survival. Li et al[17] remarked that the expression of PLK4 was enhanced in breast cancer tissues and high PLK4 expression and led to a high rate of lymph node metastasis and surrounding recurrence. Zih et al[19] manifested that PLK4 could enhance cancer cell motility via Rho GTPase activation. Mihaela et al[20] observed that Nek2 and Plk4 kinases served as crucial regulators of mitotic processes and synergized to promote breast tumorigenesis; whereas the influence of PLK4 on NB needs further exploration.

In this study, we identified the expression of SNHG1 and PLK4 in NB tissues and cells. In addition, the interaction of SNHG1 and miR-338-3p, PLK4 and miR-338-3p was confirmed. Furthermore, the functional analyses revealed the regulatory mechanism of SNHG1/miR-338-3p/PLK4 axis in NB cells. This provides a promising strategy for NB treatment.

Patients and Methods

Tissue Samples and Cell Culture

This study was approved by the Neonatal Surgery, Xuzhou City Children's Hospital Ethics Committee. All patients' parents or their guardians signed an informed consent form before surgery. A total of 33 neuroblastoma tissues and adjacent normal tissues were collected from the Neonatal Surgery, Xuzhou City Children's Hospital. All samples were frozen in liquid nitrogen after removing and stored at -80°C condition.

The human neuroblastoma cell lines (SK-N-SH, SK-N-AS) and human umbilical vein endothelial cells (HUVEC) were purchased from the American Type Culture Collection (ATCC; Manassas, VA, USA). All cells were cultured in Dulbecco's Modified Eagle's Medium (DMEM; Invitrogen, Carlsbad, CA, USA) supplemented with 10% fetal bovine serum (FBS; Invitrogen, Carlsbad, CA, USA), 100 IU/mL penicillin sodium (Gibco, Grand Island, NY, USA), and 100 microg/mL streptomycin sulfate (Gibco) at 37°C in a humidified incubator, containing 5% CO_2.

Cell Transfection

SiRNAs specifically targeting SNHG1 (si-SNHG1) and negative control (si-NC) were synthesized by GenePharma (Shanghai, China). MiR-338-3p mimics (miR-338-3p), miR-338-3p negative control (miR-NC), miR-338-3p inhibition (in-miR-338-3p), and miR-338-3p negative control inhibition (in-miR) were also purchased from GenePharma (Shanghai, China). Overexpression vector pcDNA3.1-SNHG1 (SNHG1), pcDNA3.1-PLK4 (PLK4), and empty vector (pcDNA) were purchased from RiboBio (Guangzhou, China). Cell transfection was executed by Lipofectamine™ 2000 (Thermo Fisher Scientific, Waltham, MA, USA) according to the introduction of manufacturers. Then, the transfected cells were cultured for other 48 h and used for next experiment analysis.

RNA Isolation and Reverse Transcription Quantitative Polymerase Chain Reaction (qRT-PCR)

The total RNA was extracted from sample tissues and cells by the TRIzol reagent (Invitrogen, Carlsbad, CA, USA) according to the manufacturer's protocol. The reverse transcription reactions were carried out using Transcriptor First Strand cDNA Synthesis Kit (Roche, Indianapolis, IN, USA) and then, the RNA was quickly reverse transcribed into cDNA. To perform qRT-PCR, Platinum® Quantitative PCR SuperMix-UDG kit (Thermo Fisher Scientific, Waltham, MA, USA) was used on CFX 96 Touch system (Bio-Rad, Hercules, CA, USA). Glyceraldehyde-3-phosphate dehydrogenase (GAPDH) acted as internal controls to normalize the levels. The relative expression values were calculated by the $2^{-\Delta\Delta Ct}$ method. All experiments were run in 3 repetitions. All primers were listed as follows: SNHG1: 5′-AGGCTGAAGTTACAGGTC-3′ (forward) and 5′-TTGGCTCCCAGTGTCTTA-3′ (reverse); PLK4: 5′-AATCAAGCACTCTCCAATC-3′ (forward) and 5′-TGTGTCCTTCTGCAAATC-3′ (reverse); miR-338-3p: 5′-TGCGGTCCAGCATCAGTGAT-3′ (forward) and 5′-CCAGTGCAGGGTCCGAGGT-3′ (reverse) GAPDH: 5′-CCATTTGCAGTGGCAAAG-3′ (forward) and 5′-CACCCCATTTGATGTTAGTG-3′ (reverse).

Western Blot Analysis

For Western blot, the total protein was extracted by lysis of cells with RIPA buffer (Beyotime, Shanghai, China) containing protease inhibitor. 30 μg of total protein was separated by 10% sodium dodecyl sulfate polyacrylamide gel electrophoresis (SDS-PAGE) and electro-transferred onto a polyvinylidene difluoride (PVDF) membrane. The membranes were experienced blockage with 5% skim milk in TBS buffer for 2 hours at room temperature and incubated with specific primary antibodies for target gene at 4°C overnight. The subsequent incubation at next day was performed with horseradish peroxidase (HRP)-conjugated secondary antibody. The protein signal was finally visualized using Pierce enhanced chemiluminescence (ECL) Plus Western blotting substrate (Life Technology, Carlsbad, CA, USA). Visualization of β-actin expression acted as a loading control.

The antibodies used in this study were PLK4 (1:1000; ProteinTech Group, Inc., Chicago, IL, USA), Akt (1:1000; Cell Signaling Technology, Danvers, MA, USA), p-Akt (1:1000; Cell Signaling Technology, Danvers, MA, USA), and anti-β-actin (1:5,000; Sigma-Aldrich, St. Louis, MO, USA).

Luciferase Reporter Assay

The prediction of binding sites was operated by DIANA TOOL online software. The wild-type SNHG1 (SNHG1-WT) harboring miR-338-3p potential target-binding sequences was synthesized and constructed onto pGL3 Luciferase reporter vector by Hanbio Biotechnology Co., Ltd. (Shanghai, China). Also, the mutant SNHG1 (SNHG1-MUT) reporter vector with mutant miR-30c binding sites was constructed. Then, SK-N-SH and SK-N-AS cells were harvested and co-transfected with SNHG1-WT or SNHG1-MUT, together with miR-338-3p mimics or miR-NC using Lipofectamine 2000 (Invitrogen, Carlsbad, CA, USA) in accordance with the manufacturer's instructions, respectively. 48 hours later, the cells were detected using the Dual-Luciferase assay system (Promega, Madison, WI, USA).

The interaction between 3′-UTR of PLK4 and miR-338-3p was also confirmed *via* Luciferase activity assay. All methods were the same as above: Luciferase reporter vector containing wild type PLK4 3'UTR (PLK4 3'UTR-WT) with the putative miR-338-3p target sites or mutant PLK4 3'UTR (PLK4 3'UTR-MUT) with mutation of the putative miR-338-3p target sites.

RIP Assay

Magna RIP RNA-binding Protein Immunoprecipitation Kit (Millipore, Billerica, MA, USA) was selected to perform RIP assay referring to the protocol of manufacturer. First, SK-N-SH and SK-N-AS cells transfected with miR-338-3p or miR-NC were collected and lysed by RIP lysis buffer containing protease inhibitor and RNase inhibitor. Next, 100 µl cell lysate was incubated with RIP buffer containing magnetic beads coated with antibodies against argonaute2 (Ago2; Millipore, Billerica, MA, USA) or normal mouse IgG (control; Millipore, Billerica, MA, USA) for 6 h, 4°C. Finally, qRT-PCR was performed to detect the enrichment of SNHG1.

MTT Assay

Transfected cells were seeded in 96-well plates (Corning, Corning, NY, USA) at a density of 3.0×10^3 cells per well. Then a total of 20 µl MTT solution (Sigma-Aldrich, St. Louis, MO, USA) was added into each well, and cells were incubated for 4 h at 37°C. After that, upper medium was discarded and dimethyl sulfoxide (DMSO; Sigma-Aldrich, St. Louis, MO, USA) was added to dissolve the formazan crystal in cell. Last the optical density (OD) value in each well was measured using Multiskan Ascent (Thermo Fisher Scientific, Waltham, MA, USA) at 0, 24, 48, and 72 h to value cell proliferation.

Transwell Assay

The migration and invasion assays were carried out with transwell chambers containing 6.5 mm polycarbonate membranes with 8.0 µm pores (Corning, Corning, NY, USA). The transfected cells were plated into the upper of a chamber pre-coated with matrigel matrix (BD Biosciences, Franklin Lakes, NJ, USA) for 2 h, and then, the Dulbecco's Modified Eagle's Medium (DMEM) medium supplemented with 10% fetal bovine serum (FBS) was added into the lower part of the chamber. After incubation at 37°C in 5% CO_2 for 30 h, the cells at lower surface of the membrane were fixed with methanol for 30 min and stained with 0.1% crystal violet for 30 min at room temperature. Next, cell migration and invasion were examined by light microscopy (Olympus, Tokyo, Japan).

Nude Mouse Tumorigenicity Assay In Vivo

The animal experiments were approved by the Animal Care and Use Committee of Neonatal surgery, Xuzhou City Children's Hospital. For xenograft experiments, six-week-old male athymic nude mice (n=5 per group) were purchased from Shanghai Experimental Animal Center (Shanghai, China). Lentiviral vector (Lenti-short hairpin sh-SNHG1) for stable SNHG1 down-expression was obtained from Genechem (Shanghai, China). Mice were injected subcutaneously in the upper back with 1×10^6 tumor cells stably transfected with sh-SNHG1 or sh-NC. The Vernier caliper was used to measure tumor volume once a week. After one month, mice were sacrificed and examined for next experiments, including tumor weight and gene expression.

Statistical Analysis

All experiments above were repeated 3 times. All quantitative data were analyzed by SPSS 21.0 (IBM Corp., Armonk, NY, USA) and date were shown as mean ± standard error of mean. The differences for the two sets of data or multiple sets of data were analyzed by Student's *t*-tests and One-way analysis of variance (ANOVA), respectively. The post-hoc test used to validate ANOVA for pairwise comparisons was Tukey's test. The differences were considered statistically significant at $p < 0.05$.

Results

SNHG1 Was Significantly Increased in Neuroblastoma Tissues and Cells

Expression of SNHG1 was measured using qRT-PCR. Notably, SNHG1 was upregulated in NB compared with adjacent normal tissue (Figure 1A). Meanwhile, the result of SNHG1 expression deemed that there was a prominently accumulation in NB cells SK-N-SH and SK-N-AS other than in normal cell HUVEC (Figure 1C). This indicated that SNHG1 played a crucial role in the development of NB. Besides, Kaplan-Meier

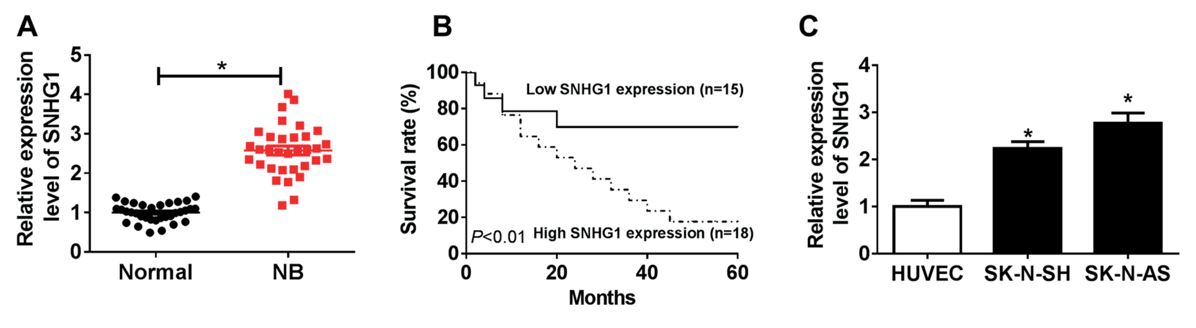

Figure 1. The expression of SNHG1 in NB tissues and cell lines and the analysis of survival rate with SNGH1 high expression or low expression. **A,** Expression of SNHG1 in 33 NB tissues was higher than in adjacent normal tissues. **B,** The survival rate of NB patients with high SNHG1 expression was significantly lower than patients with low SNHG1 expression within five years. **C,** Expression of SNHG1 in human NB cell lines SK-N-SH and SK-N-AS was higher than that in human umbilical vein endothelial cells (HUVEC). $^*p<0.05$.

survival analysis was applied to detect the putative effect of SNHG1 on the survival rate of NB patients, and the results showed that the mortality of 18 patients with high SNHG1 expression outclassed 15 patients with low SNHG1 expression (Figure 1B). All data indicated that SNHG1 might serve as carcinogenic role in NB.

SNHG1 Exercised its Role by Targeting MiR-338-3p

To find out the relationship between SNHG1 and miR-338-3p, the potential binding sites were predicted *via* online software Diana tools. As shown in Figure 2A, sequence alignment displayed that SNHG1 contained binding sites with miR-338-3p. In addition, Luciferase reporter assay indicated that miR-338-3p pronouncedly diminished Luciferase activity in SK-N-SH and SK-N-AS co-transfected SNHG1-WT and miR-338-3p mimic; however, the Luciferase activity in SK-N-SH and SK-N-AS co-transfected with miR-203 mimic and SNHG1-MUT manifested no difference compared with the control (Figures 2B and 2C). Moreover, RIP assay was carried out and made a clear result that miR-338-3p mimic could strengthen the enrichment of SNHG1 in Ago2 RIP, whereas its efficacy was declined rapidly in response to IgG RIP (Figure 2D). Next, we measured the expression of miR-338-3p in NB tissues and cells. As indicated in Figure 2E, a marked weakening of expression level existed in NB tissues compared with normal tissues. Not surprisingly, the expression of miR-338-3p in SK-N-SH and SK-N-AS was lower than that in HUVEC (Figure 2F). The correlation analysis found that SNHG1 expression was negatively correlated with miR-338-3p expression (Figure 2G). As we observed in Figure 2H and 2I, the expression of SNHG1 was abundant when the cells transfected with pcDNA-SNHG1, while the level of miR-338-3p was decreased. On the contrary, the expression of SNHG1 was down and the expression of miR-338-3p was increased in SK-N-SH and SK-N-AS transfected with si-SNHG1. These data suggested that SNHG1 competitively bound to miR-338-3p and targetedly inhibited the expression of miR-338-3p in NB cells.

The Suppression on Cell Proliferation, Migration, and Invasion of SNHG1 Down-Regulation Could Be Rescued Through MiR-338-3p Inhibition

A certain number of experiments were performed to investigate the possible effects of SNHG1 and miR-338-3p on NB cell proliferation, migration, and invasion. MTT assay showed that the proliferation of SK-N-SH (Figure 3A) and SK-N-AS (Figure 3B) cells was strongly diminished in si-SNHG1 system compared with si-NC; however, the proliferation was strengthened in si-SNHG1+in-miR-338-3p system other than in si-SNHG1+in-338-3p-NC. Flow cytometry concluded that an apparent decline of cell migration occurred in SK-N-SH and SK-N-AS with si-SNHG1 group compared with control, whereas, si-SNHG1+in-miR-338-3p group could restore cell migration ability inhibited by si-SNHG1 (Figure 3C). As for cell invasion, the representation consistent with cell migration was shown in Figure 3D. Figure 3E remarked these relationships in which si-SNHG1 hold a negative effect on p-AKT expression compared with si-NC, and si-SNHG1+in-miR-338-3p enhanced p-AKT expression in NB cells compared with si-SNHG1+in-miR-338-3p-NC. All data above remarked that SNHG1 knockdown could suppress cell viability, migration, and invasion by enhancing the expression of miR-338-3p in NB cells.

PLK4 Was a Target of MiR-338-3p and Was Upregulated in NB Tissues and Cells

Fortunately, the prediction of online software Diana tools also showed that miR-338-3p might bind to 3′-UTR of PLK4 mRNA (Figure 4A). Meanwhile, Luciferase reporter assay demonstrated that the co-transfection of SK-N-SH and SK-N-AS cells with miR-338-3p mimics and PLK4 3’UTR-WT reporter construct suppressed the Luciferase activity, as compared to NC transfected cells. However, the activity of the reporter construct mutated specific miR-338-3p target sites was uninfluential (Figure 4B and 4C). Then, the relative expression level of PLK4 was observed in NB cells and tissues by using qRT-PCR. The result showed that PLK4 expression was higher in tumor tissues than that in normal tissues (Figure 4D), which was consistent with the analysis in NB cells SK-N-SH and SK-N-AS (Figure 4E). The correlation analysis declared that the PLK4 expression was negatively associated with miR-338-3p (Figure 4F). Eventually, the expression of PLK4 in SK-N-SH and SK-N-AS transfected with miR-338-3p mimic and miR-338-3p-NC was measured from mRNA level and protein level. As displayed in Figure 4G, PLK4 expression was strikingly faint when miR-338-3p was upregulated. The

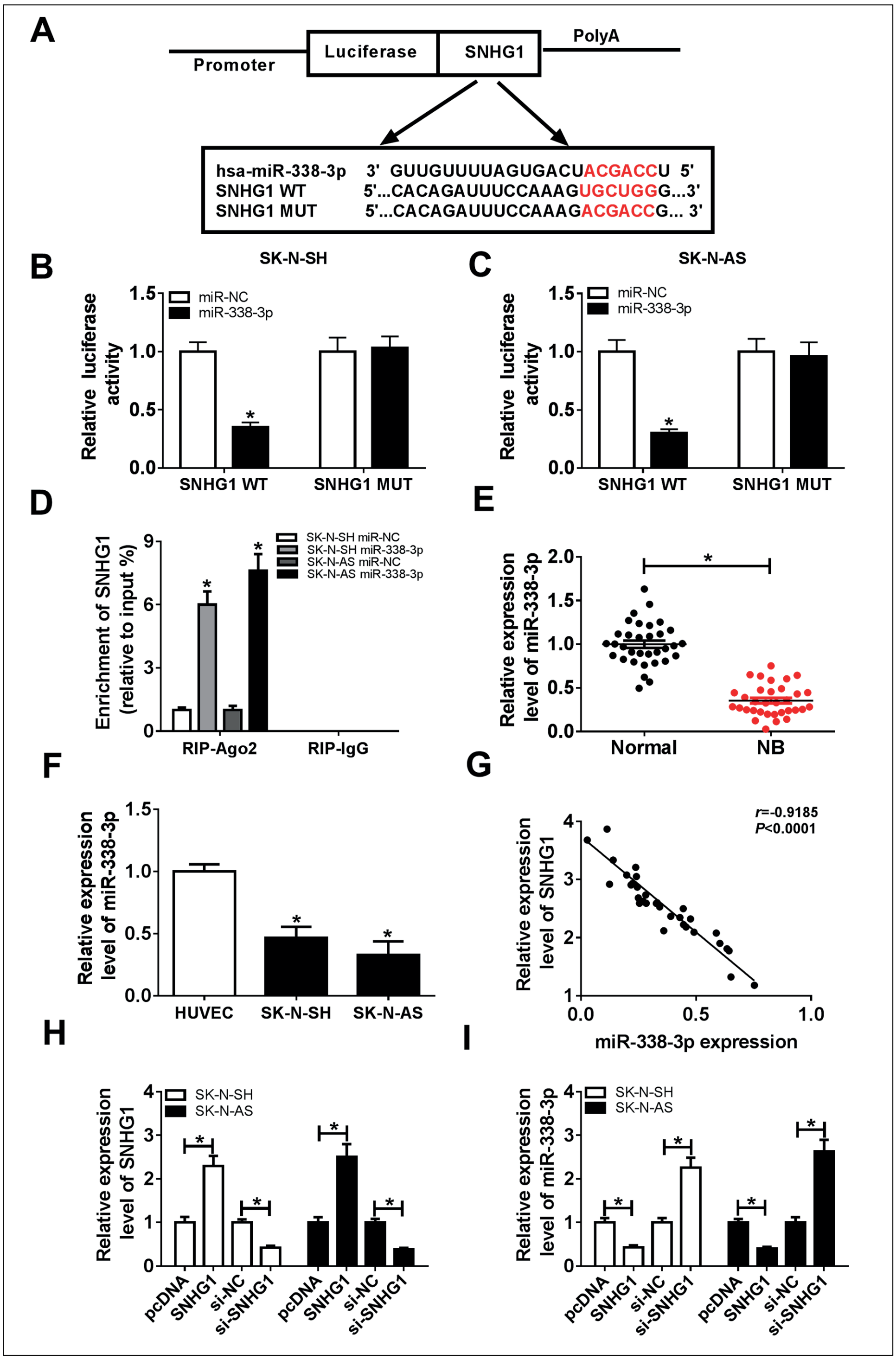

Figure 2. SNHG1 directly bound with miR-338-3p and served as a sponge for miR-338-3p. **A,** Prediction online showed that miR-338-3p had potential binding sites with SNHG1. **B,** and **C,** Interaction between SNHG1 and miR-338-3p was determined by Luciferase reporter assay in SK-N-SH and SK-N-AS. **D,** Interaction between SNHG1 and miR-338-3p was detected by RIP assay. **E,** The result of qRT-PCR suggested that the expression of miR-338-3p in NB tissues was decreased compared with that in normal tissues. **F,** The expression of miR-338-3p in SK-N-SH and SK-N-AS was lower than in HUVEC. **G,** The negative correlation between miR-338-3p and SNHG1 expression in NB. **H**, In SK-N-SH and SK-N-AS, the expression of SNHG1 was increased when the cells transfected with pcDNA-SNHG1, while the expression was reduced when cells transfected with si-SNHG1. **I,** In SK-N-SH and SK-N-AS, the expression of miR-338-3p was increased when cells transfected with si-SNHG1, while the expression was reduced when cells transfected with pcDNA-SNHG1. $^*p<0.05$.

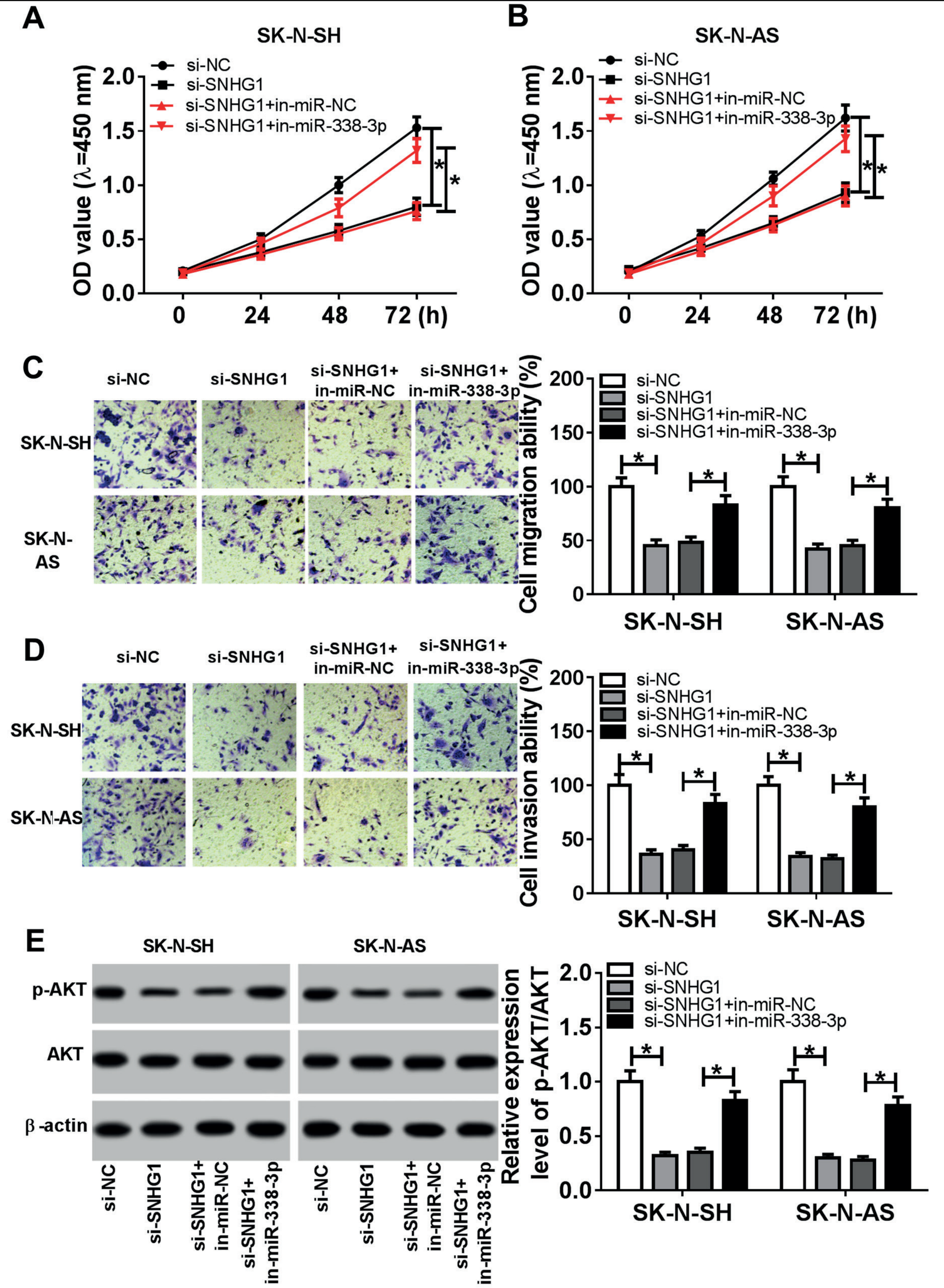

Figure 3. MiR-338-3p inhibition reversed the effect of SNHG1 knockdown on cell proliferation, migration and invasion in SK-N-SH and SK-N-AS. **A,** and **B,** The proliferation of SK-N-SH and SK-N-AS cells transfected with si-SNHG1 or si-SNHG1+in-miR-338-3p was detected at the regular time by MTT. **C,** and **D,** Transwell analysis was performed to detect cell migration and invasion of SK-N-SH and SK-N-AS cells transfected with si-SNHG1 or si-SNHG1+in-miR-338-3p (100×). **E,** The expression of p-Akt was measured by Western-blot in SK-N-SH and SK-N-AS cells transfected with si-SNHG1 or si-SNHG1+in-miR-338-3p, respectively. *$p<0.05$.

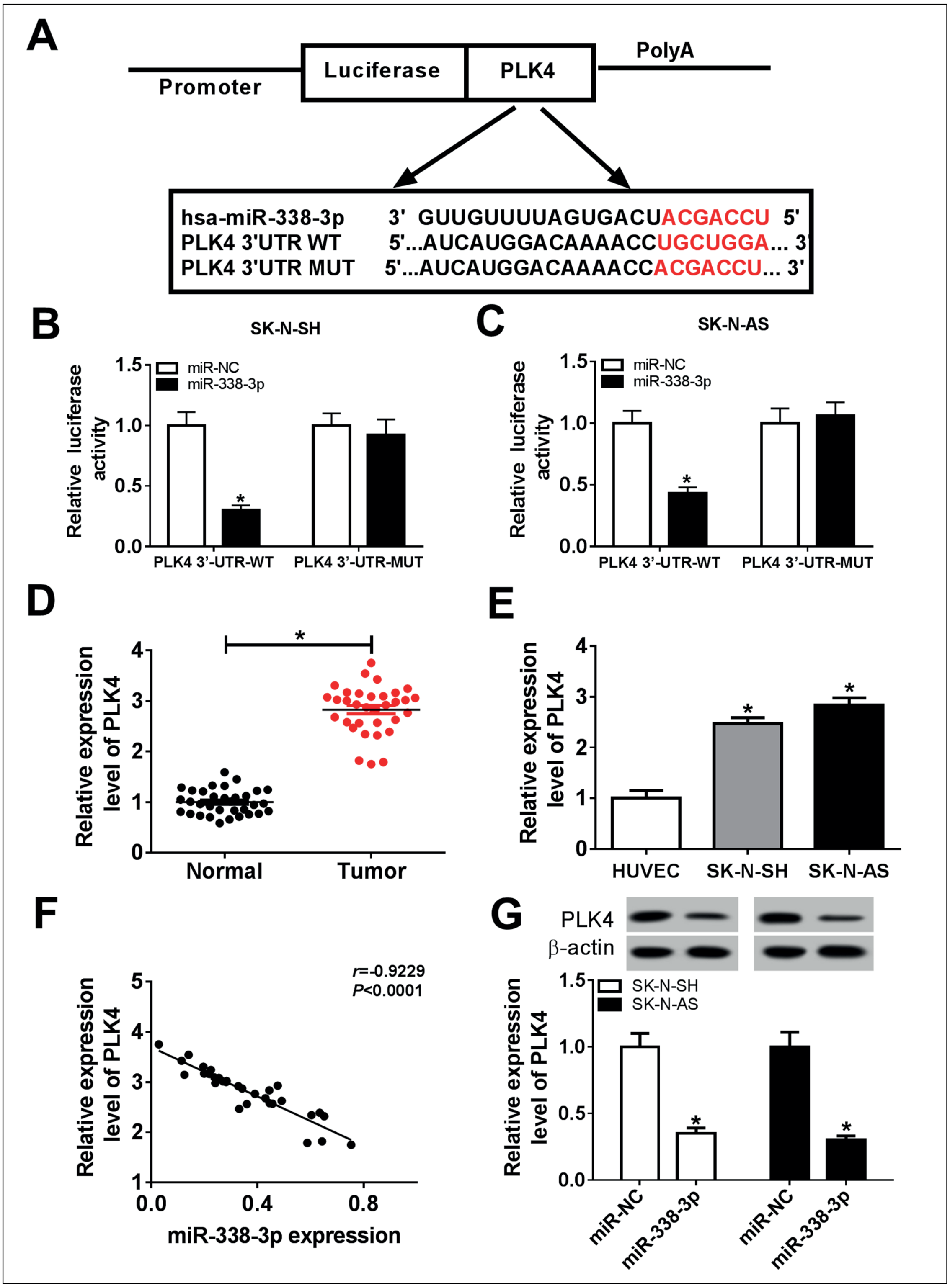

Figure 4. MiR-338-3p regulated the expression of PLK4 by targeting it. **A,** The putative binding sites were predicted between PLK4 and miR-338-3p through online software DIANA TOOL. **B,** and **C,** Luciferase activity reporter assay confirmed the relationship between PLK4 and miR-338-3p in SK-N-SH and SK-N-AS cells. **D,** and **E,** The expression of PLK4 was detected by qRT-PCR in NB tissues and cell lines. **F,** There was a negative correlation of miR-338-3p and PLK4 mRNA in NB cells. **G,** The expression level of PLK4 was examined by Western-blot and qRT-PCR from protein level and mRNA level in SK-N-SH and SK-N-AS cells. *$p<0.05$.

result indicated that miR-338-3p regulated PLK4 expression by directly binding to the 3'UTR sequence of PLK4 mRNA.

The Inhibited Effect of MiR-338-3p Mimic on Cell Proliferation, Migration, and Invasion Could Be Overturned Through PLK4 Upregulating in NB Cells

To clarify the influence of miR-338-3p and PLK4 in NB cells, SK-N-SH and SK-N-AS was transfected with miR-338-3p mimic or miR-338-3p mimic+pCDNA-PLK4. MTT assay showed that miR-338-3p mimic resulted in a substantial decrease of the rate of proliferation compared with control; however, the proliferation of cells with miR-338-3p mimic+pCDNA-PLK4 group was recovered (Figures 5A and 5B). Cell migrated ability of miR-338-3p mimic NB cells was significantly shorter than that of miR-338-3p-NC NB cells; nevertheless, NB cells transfected

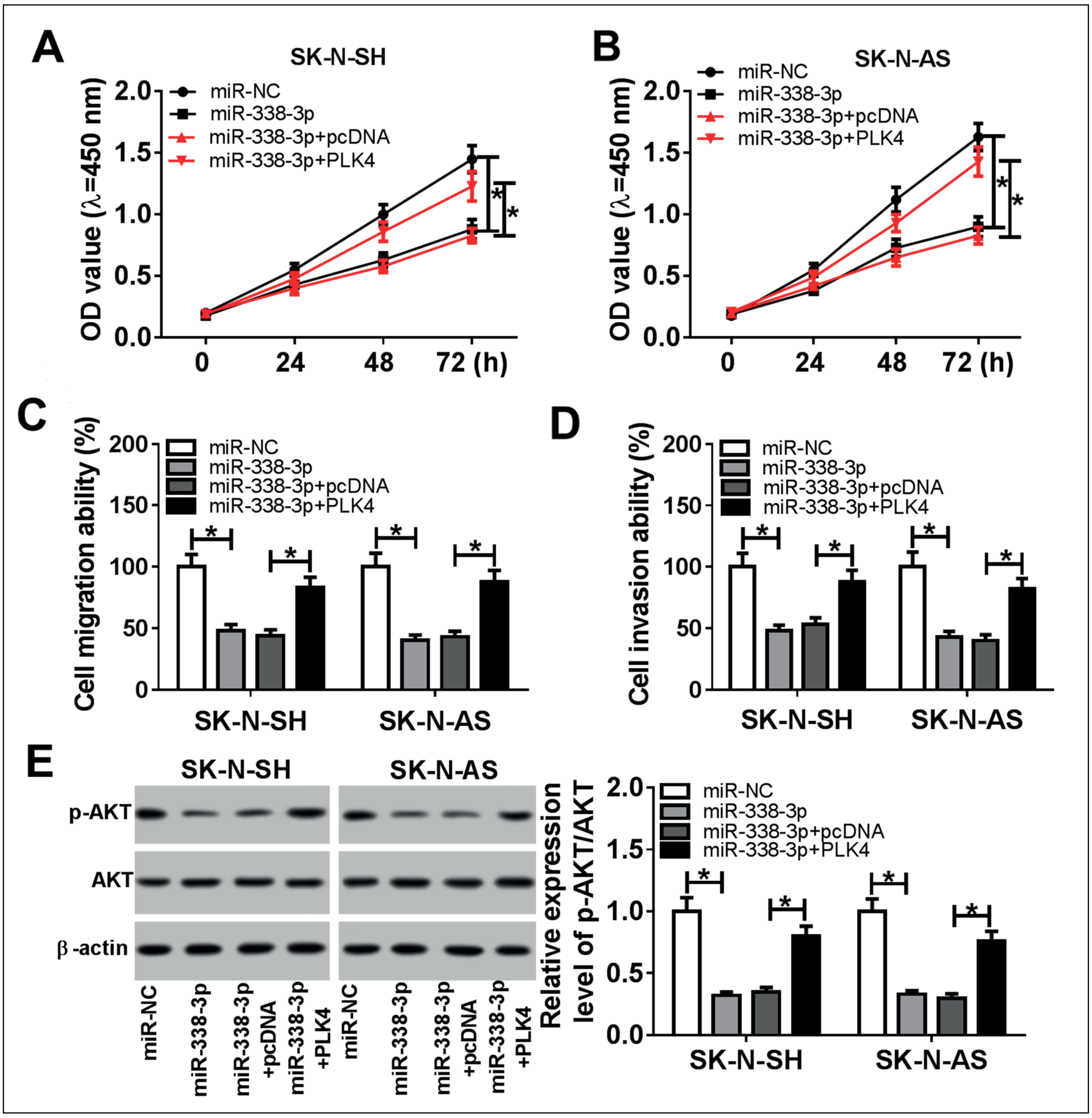

Figure 5. PLK4 upregulation reversed the influence on cell proliferation, migration, and invasion of miR-338-3p enrichment. **A,** and **B,** The proliferation of SK-N-SH and SK-N-AS cells transfected with miR-338-3p mimic or miR-338-3p mimic+pcDNA-PLK4 was calculated by MTT assay. **C,** and **D,** Transwell analysis was performed to detect cell migration and invasion of SK-N-SH and SK-N-AS cells transfected with miR-338-3p mimic or miR-338-3p mimic+pcDNA-PLK4. **E,** The expression of p-Akt was identified by Western-blot in SK-N-SH and SK-N-AS cells transfected with miR-338-3p mimic or miR-338-3p mimic+pcDNA-PLK4. *p<0.05.

with miR-338-3p mimic+pCDNA-PLK4 group had an intensified cell migration ability other than miR-338-3p mimic+pCDNA control (Figure 5C). Similar experiments were performed in cell invasion (Figure 5D). We also measured the change of p-AKT/AKT expression in SK-N-SH and SK-N-AS transfected with miR-338-3p mimic or miR-338-3p mimic+pCDNA-PLK4, respectively. According to Figure 5E, the expression of p-AKT was dramatically decreased in the cells transfected miR-338-3p mimic. Expectedly, a growing tendency of p-AKT expression occurred in cells transfected with miR-338-3p mimic+pCDNA-PLK4 compared with the control. These data suggested that miR-338-3p affluence depleted cell proliferation, migration, and invasion by sequestering the expression of PLK4.

SNHG1 Regulated PLK4 Expression Through Targeting MiR-338-3p

The expression of PLK4 was appraised from mRNA and protein levels in SK-N-SH and SK-N-AS with si-ANHG1 group, si-NC, si-ANHG1+in-miR-338-3p group or si-ANHG1+in-miR-338-3p-NC. QRT-PCR analysis showed that SNHG1 knockdown significantly reduced the expression level of PLK4, whereas miR-338-3p inhibition reversed this negative effect of SNHG1 knockdown in NB cells compared with the negative control (Figure 6A). In terms of protein level, Western-blot exhibited the uniform consequence in Figure 6B. The data defined that SNHG1 had ability to act on the expression of PLK4 *via* targeting miR-338-3p.

SNHG1 Knockdown Declined Tumor Growth of NB In Vivo

To determine the effect of SNHG1 on the tumor growth *in vivo*, SK-N-SH cell was transfected sh-SNHG1 and sh-NC and inoculated into subcutaneous tissues of athymic nude mice. After few weeks, the volume and weight of mice tumor were recorded. As shown in Figure 7A and 7B, SNHG1 downregulation significantly cut down the volume and weight of tumor compared with negative control. qRT-PCR analysis illustrated that SNHG1 expression was prominently lower in tumor tissues with sh-SNHG1 group than sh-NC group (Figure 7C), and miR-338-3p expression was signally improved in sh-SNHG1 group compared with the control (Figure 7D). Western-blot analysis explained that PLK4 level was decreased in SNHG1 knockdown SK-N-SH cell compared with that in the control (Figure 7E). In addition, the expression of p-AKT/AKT was also measured in this system (Figure 7F). Compared to control, p-AKT/AKT expression was markedly declined in cell transfected with sh-SNHG1 group. Thus, it was concluded that SNHG1 down-expression prejudiced tumor formation and growth *in vivo.*

Discussion

Neuroblastoma is a heterogeneous tumor deriving from neural crest progenitor cells[21]. Neuroblastoma is extremely unfriendly to individuals diagnosed at over 18 months of age with poor prognosis, highly heterogeneous clinical behav-

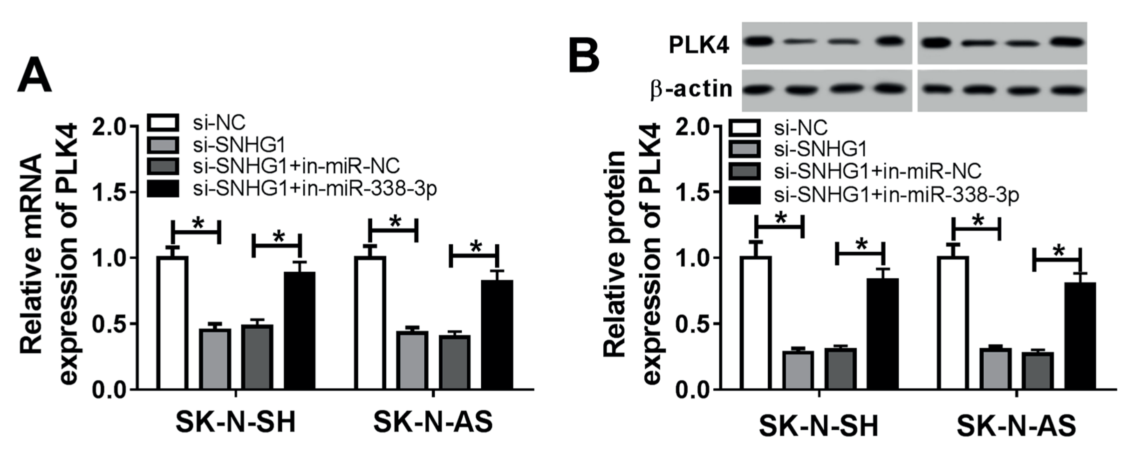

Figure 6. The mRNA and protein expression levels of PLK4 were measured in SK-N-SH and SK-N-AS cells with si-SNHG1 group or si-SNHG1+in-miR-338-3p group. **A,** PLK4 downregulated in cells transfected with si-SNHG1, while PLK4 upregulated in cells transfected with si-SNHG1+in-miR-338-3P. **B,** The result was similar with (**A**) from protein level. *$p<0.05$.

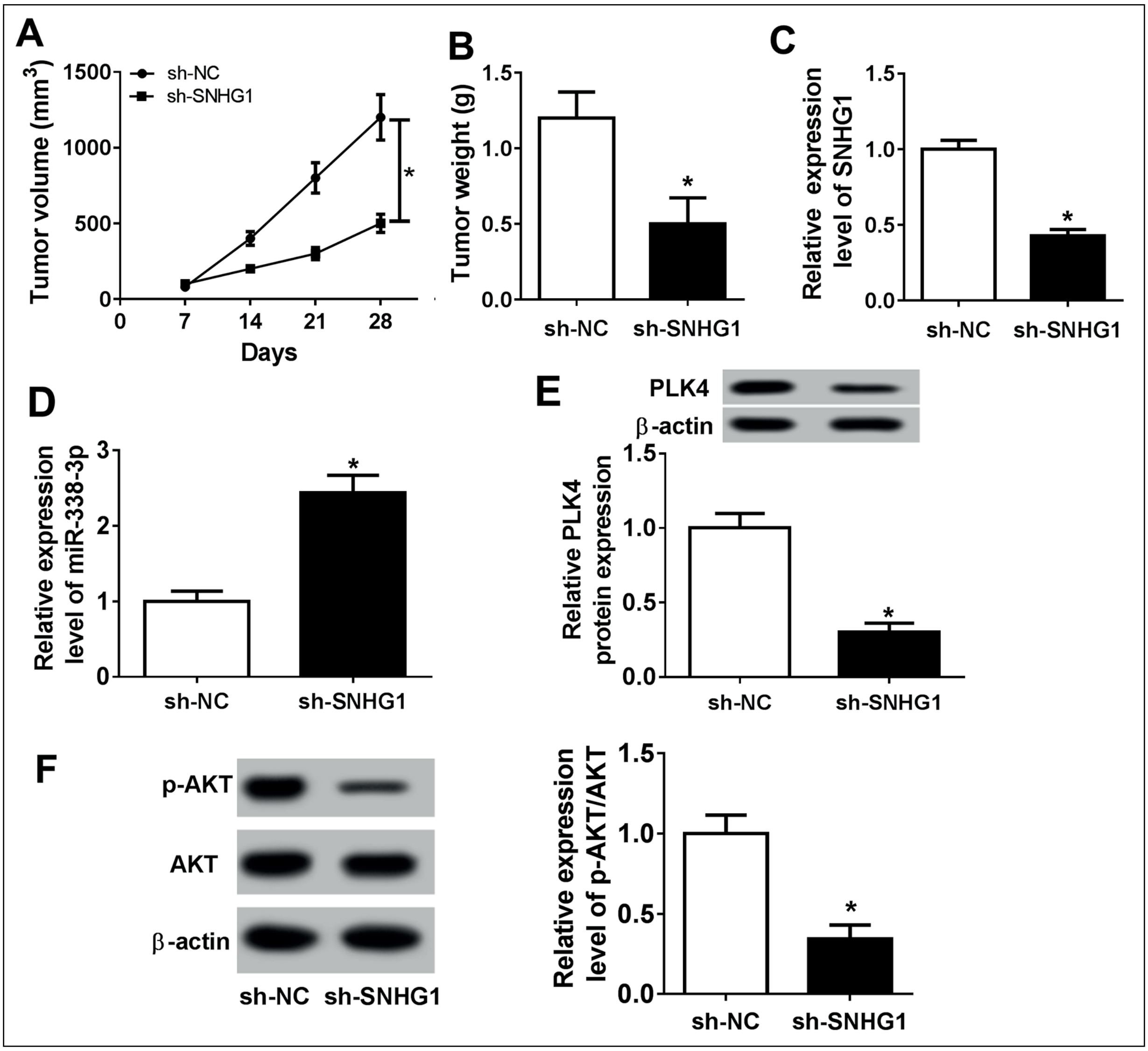

Figure 7. SNHG1 knockdown suppressed the growth of tumor *in vivo*. **A,** Tumor volume was recorded per week after inoculating of sh-SNHG1 and sh-NC. **B,** Tumor weight was measured at last. **C-D,** and **E,** The expression of SNHG1, miR-338-3p, and PLK4 was detected in xenografted tumors, respectively. **F,** The expression of p-Akt was observed by Western-blot in xenografted tumors. *$p<0.05$.

ior, intricate metastatic processes[1,22]. Nowadays, about half of all diagnosed cases are served as disease with high-risk relapse, while overall survival rates remain pessimistic, less than 40% at 5 years[23]. LncRNAs emphasized the role of these regulatory RNAs as promising drug targets for therapeutic interventions[22]. In our study, we identified the role of lncRNA SNHG1 in NB cells, and verified the relationship between miR-338-3p and SNHG1 or PLK4. Besides, we first provided the view on the carcinogenic role of SNHG1 and elucidated the network of SNHG1/miR-338-3p/PLK4 functioning in NB. Sahu et al[24] revealed that SNHG1 was highly expressed in NB through co-expression analysis and was verified by qRT-PCR. The result above was consistent with our study and these data suggested that SNHG1 exhibits vital roles in NB development. In addition, it is known that lncRNAs can act as specific ceRNAs to regulate the expression of the downstream miRNAs. Recently, the research of many miRNAs targeted by lncRNA SNHG1 to regulate the growth and development of cancer cells have been reported. For instance, SNHG1 acted as a non-degradable sponge for miR-338 to promote cell proliferation in esophageal cancer cells[25]. SNHG1 was able to directly bind to miR-15-5p and repress miR-15-5p expression, which activated SIAH1 in human neuroblastoma SH-SY5Y cells[26]. SNHG1 strengthened CDK7 expression by competitively targeting miR-199a-3p, and then promoted cell proliferation and cell cycle progression in prostate cancer[27]. Hence, in our study, we first illustrated the interaction of SNHG1 and miR-338-3p through prediction online, authentication of Luciferase reporter assay and RIP assay and we substantiated that miR-338-3p could be targeted by SNHG1, leading to consequent reactions in NB. Chen et al[28] showed that miR-338-3p expression levels had an average of 36% decrease in metastatic tumor tissues compared with paired primary tumor tissues, which was in accordance with our research, suggesting it has a role in the progression of NB. Statistics show that ectopic expression of miRNA is closely related to tumor cell proliferation, invasion, metastasis, tumor growth, and apoptosis[29]. The role of miRNAs usually depends on what genes they target[25]. Up to now, it has been reported that miR-338 directly targeted proto-oncogenes smoothened (SMO) in liver cancer[12], phosphatidylinositol-3,4,5-trisphosphate-dependent Rac exchange factor 2 (PREX2a) in neuroblastoma[28], and synovial sarcoma, X breakpoint 2 interacting protein (SSX2IP) in gastric cancer[30], respectively. In our study, we predicted and verified PLK4 as a target gene of miR-338-3p in NB cells. Functional analyses implied that miR-338-3p upregulation could inhibit the expression of PLK4 and phosphorylation of protein kinase B (p-Akt).

Ackermann et al[31] showed that the expression level of PLK1 in NB tissues and NB cell lines was remarkably upregulated, and its expression was always associated with poor prognostic markers. Weichert et al[32] showed that PLK1 and PLK 3 overexpression invariably occurred in highly proliferating malignant epithelial ovarian tumors and their overexpression was connected with mitosis and worse prognosis. This suggested that PLK was active in tumorigenesis and metastasis, was always a damage for prognosis, and could be a potential tumor-promoting factor in NB. Tian et al[16] demonstrated that PLK4 was highly expressed in NB tissues, which was consistent with the results in this research. We also found that there was a negative correlation of expression between PLK4 and miR-338-3p. Cell proliferation, migration, and invasion assay showed that PLK4 could break the inhibition of miR-338-3p accumulation in NB cells. Further, PLK4 had the ability to enhance the expression of p-Akt inhibited by miR-338-3p affluence.

Conclusions

It has been demonstrated that SNHG1 promoted proliferation, migration, and invasion by downregulating miR-338-3p and upregulating PLK4 in NB cells, which may exhilaratingly provide some potential therapeutic targets or diagnostic markers for NB treatment. However, the molecular mechanisms of cancer development and metastasis are anfractuous and elusive, and need to be further explored.

Conflict of Interest

The Authors declare that they have no conflict of interests.

Ethics Approval and Consent to Participate

This study was approved by the Ethics Committee of XuZhou Children's Hospital. The methods used in this study were performed in accordance with relevant guidelines and regulations. Written consent was obtained from the participants or guardians of participants under 16 years old.

Availability of Data and Materials

All original data and materials are available from the corresponding author upon request

References

1) Maris JM. Recent advances in neuroblastoma. N Engl J Med 2010; 362: 2202-2211.
2) Jiang M, Stanke J, Lahti JM. The connections between neural crest development and neuroblastoma. Curr Top Dev Biol 2011; 94: 77-127.
3) Maris JM. The biologic basis for neuroblastoma heterogeneity and risk stratification. Curr Opin Pediatr 2005; 17: 7-13.
4) Brodeur GM. Neuroblastoma: biological insights into a clinical enigma. Nat Rev Cancer 2003; 3: 203-216.
5) Li H, Ma SQ, Huang J, Chen XP, Zhou HH. Roles of long noncoding RNAs in colorectal cancer metastasis. Oncotarget 2017; 8: 39859-39876.
6) Thin KZ, Tu JC, Raveendran S. Long non-coding SNHG1 in cancer. Clin Chim Acta 2019; 494: 38-47.

7) Zhang M, Wang W, Li T, Yu X, Zhu Y, Ding F, Li D, Yang T. Long noncoding RNA SNHG1 predicts a poor prognosis and promotes hepatocellular carcinoma tumorigenesis. Biomed Pharmacother 2016; 80: 73-79.

8) Yang H, Wang S, Kang YJ, Wang C, Xu Y, Zhang Y, Jiang Z. Long non-coding RNA SNHG1 predicts a poor prognosis and promotes colon cancer tumorigenesis. Oncol Rep 2018; 40: 261-271.

9) Cui Y, Zhang F, Zhu C, Geng L, Tian T, Liu H. Upregulated lncRNA SNHG1 contributes to progression of non-small cell lung cancer through inhibition of miR-101-3p and activation of Wnt/β-catenin signaling pathway. Oncotarget 2017; 8: 17785-17794.

10) Sassen S, Miska EA, Caldas C. MicroRNA: implications for cancer. Virchows Arch 2008; 452: 1-10.

11) Du L, Schageman JJ, Irnov, Girard L, Hammond SM, Minna JD, Gazdar AF, Pertsemlidis A. MicroRNA expression distinguishes SCLC from NSCLC lung tumor cells and suggests a possible pathological relationship between SCLCs and NSCLCs. J Exp Clin Cancer Res 2010; 29: 75.

12) Huang XH, Chen JS, Wang Q, Chen XL, Wen L, Chen LZ, Bi J, Zhang LJ, Su Q, Zeng WT. MiR-338-3p suppresses invasion of liver cancer cell by targeting smoothened. J Pathol 2011; 225: 463-472.

13) Chen JS, Liang LL, Xu HX, Chen F, Shen SL, Chen W, Chen LZ, Su Q, Zhang LJ, Bi J, Zeng WT, Li W, Ma N, Huang XH. MiR-338-3p inhibits epithelial-mesenchymal transition and metastasis in hepatocellular carcinoma cells. Oncotarget 2016; 8: 71418-71429.

14) Huang N, Wu Z, Lin L, Zhou M, Wang L, Ma H, Xia J, Bin J, Liao Y, Liao W. MiR-338-3p inhibits epithelial-mesenchymal transition in gastric cancer cells by targeting ZEB2 and MACC1/Met/Akt signaling. Oncotarget 2015; 6: 15222-15234.

15) Swallow CJ, Ko MA, Siddiqui Nu, Hudson JW, Dennis JW. Sak/Plk4 and mitotic fidelity. Oncogene 2005; 24: 306-312.

16) Tian X, Zhou D, Chen L, Tian Y, Zhong B, Cao Y, Dong Q, Zhou M, Yan J, Wang Y, Qiu Y, Zhang L, Li Z, Wang H, Wang D, Ying G, Zhao Q. Polo-like kinase 4 mediates epithelial-mesenchymal transition in neuroblastoma via PI3K/Akt signaling pathway. Cell Death Dis 2018; 9: 54.

17) Li Z, Dai K, Wang C, Song Y, Gu F, Liu F. Expression of polo-like kinase 4(PLK4) in breast cancer and its response to taxane-based neoadjuvant chemotherapy. J Cancer 2016; 7: 1125-1132.

18) Lohse I, Mason JM, Cao PJ, Pintilie M, Bray MR, Hedley DW. Activity of the novel polo-like kinase 4 inhibitor CFI-400945 in pancreatic cancer patient-derived xenografts. Oncotarget 2017; 8: 3064-3071.

19) Zih FSW, Rosario CO, Brashavitskaya O, Kazazian K, Swallow CJ. Polo-like kinase 4 (Plk4) enhances cancer cell motility via RhoGTPase activation. J Am Coll Surg 2012; 215: S129-S130.

20) Mihaela M, Saavedra HI. Nek2 and Plk4: prognostic markers, drivers of breast tumorigenesis and drug resistance. Front Biosci (Landmark Ed.) 2014; 19: 352-365.

21) Zhuo ZJ, Zhang R, Zhang J, Zhu J, Yang T, Zou Y, He J, Xia H. Associations between lncRNA MEG3 polymorphisms and neuroblastoma risk in Chinese children. Aging (Albany NY) 2018; 10: 481-491.

22) Esposito MR, Aveic S, Seydel A, Tonini GP. Neuroblastoma treatment in the post-genomic era. J Biomed Sci 2017; 24: 14.

23) Maris JM, Hogarty MD, Bagatell R, Cohn SL. Neuroblastoma. Lancet 2007; 369: 2106-2120.

24) Sahu D, Hsu CL, Lin CC, Yang TW, Hsu WM, Ho SY, Juan HF, Huang HC. Co-expression analysis identifies long noncoding RNA SNHG1 as a novel predictor for event-free survival in neuroblastoma. Oncotarget 2016; 7: 58022-58037.

25) Yan Y, Fan Q, Wang L, Zhou Y, Li J, Zhou K. LncRNA Snhg1, a non-degradable sponge for miR-338, promotes expression of proto-oncogene CST3 in primary esophageal cancer cells. Oncotarget 2017; 8: 35750-35760.

26) Chen Y, Lian YJ, Ma YQ, Wu CJ, Zheng YK, Xie NC. LncRNA SNHG1 promotes α-synuclein aggregation and toxicity by targeting miR-15b-5p to activate SIAH1 in human neuroblastoma SH-SY5Y cells. Neurotoxicology 2018; 68: 211-221.

27) Li J, Zhang Z, Xiong L, Guo C, Jiang T, Zeng L, Li G, Wang J. SNHG1 lncRNA negatively regulates miR-199a-3p to enhance CDK7 expression and promote cell proliferation in prostate cancer. Biochem Biophys Res Commun 2017; 487: 146-152.

28) Chen X, Pan M, Han L, Lu H, Hao X, Dong Q. MiR-338-3p suppresses neuroblastoma proliferation, invasion and migration through targeting PREX2a. FEBS Lett 2013; 587: 3729-3737.

29) Hao NB, He YF, Li XQ, Wang K, Wang RL. The role of miRNA and lncRNA in gastric cancer. Oncotarget 2017; 8: 81572-81582.

30) Li P, Chen X, Su L, Li C, Zhi Q, Yu B, Sheng H, Wang J, Feng R, Cai Q, Li J, Yu Y, Yan M, Liu B, Zhu Z. Epigenetic silencing of miR-338-3p contributes to tumorigenicity in gastric cancer by targeting SSX2IP. PLoS One 2013; 8: e66782.

31) Ackermann S, Goeser F, Schulte JH, Schramm A, Ehemann V, Hero B, Eggert A, Berthold F, Fischer M. Polo-like kinase 1 is a therapeutic target in high-risk neuroblastoma. Clin Cancer Res 2011; 17: 731-741.

32) Weichert W, Denkert C, Schmidt M, Gekeler V, Wolf G, Köbel M, Dietel M, Hauptmann S. Polo-like kinase isoform expression is a prognostic factor in ovarian carcinoma. Br J Cancer 2004; 90: 815-821.